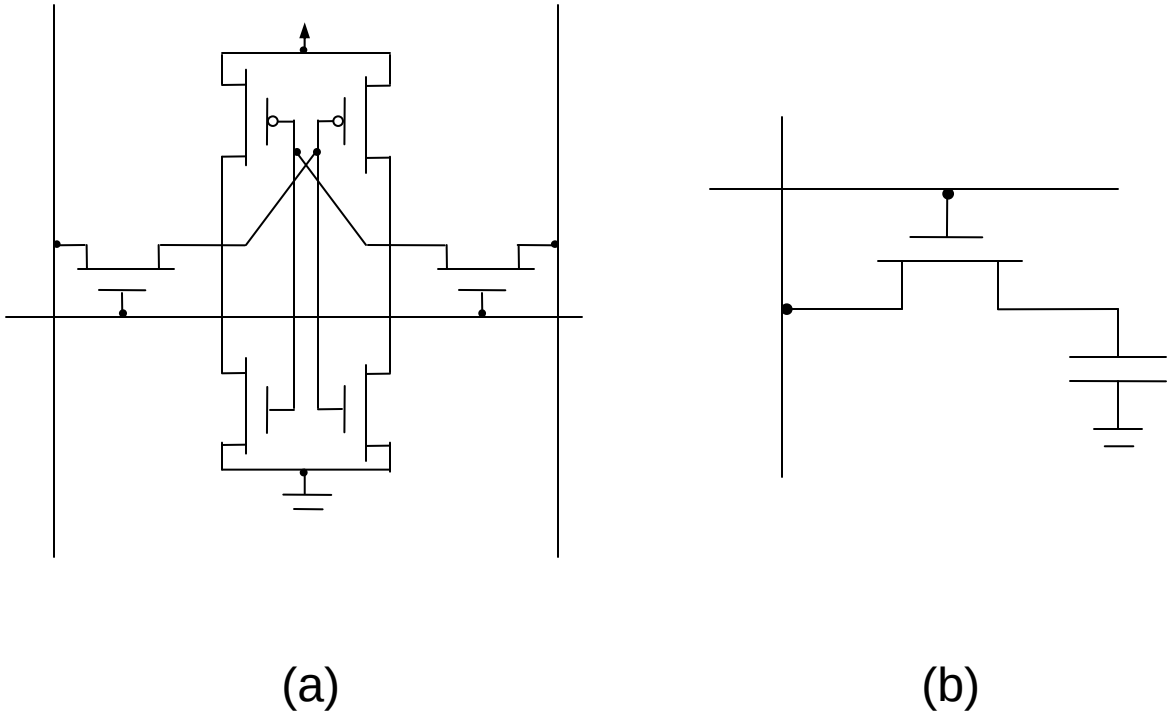

Figure 22.1 Device structures of (a) SRAM and (b) DRAM.

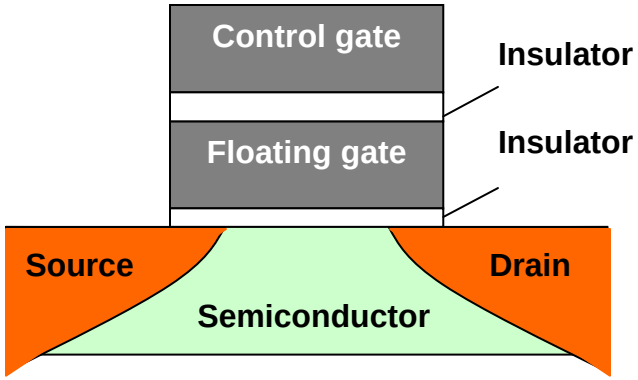

Figure 22.2 Device structures of a flash memory.

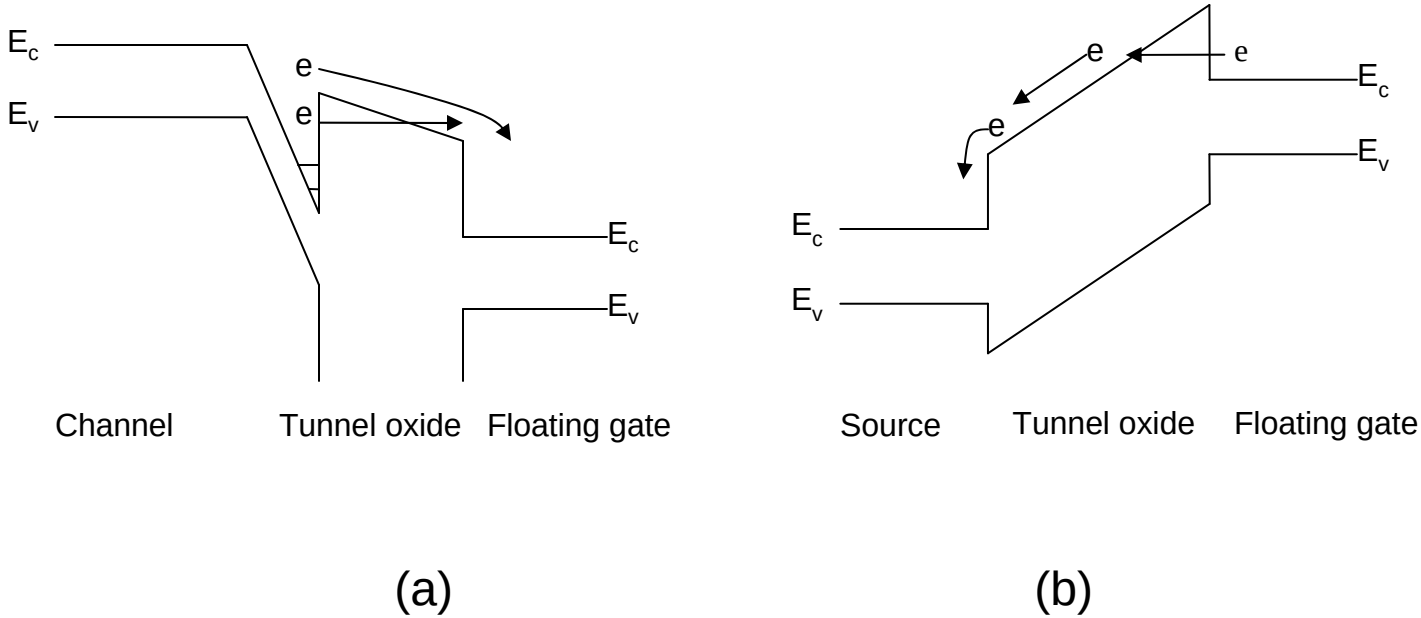

Figure 22.3 Operation mechanism of a flash memory. (a) hot electron injection from channel into the floating gate; (b) erasure process: stored electrons are released through a tunneling process from floating gate into source.

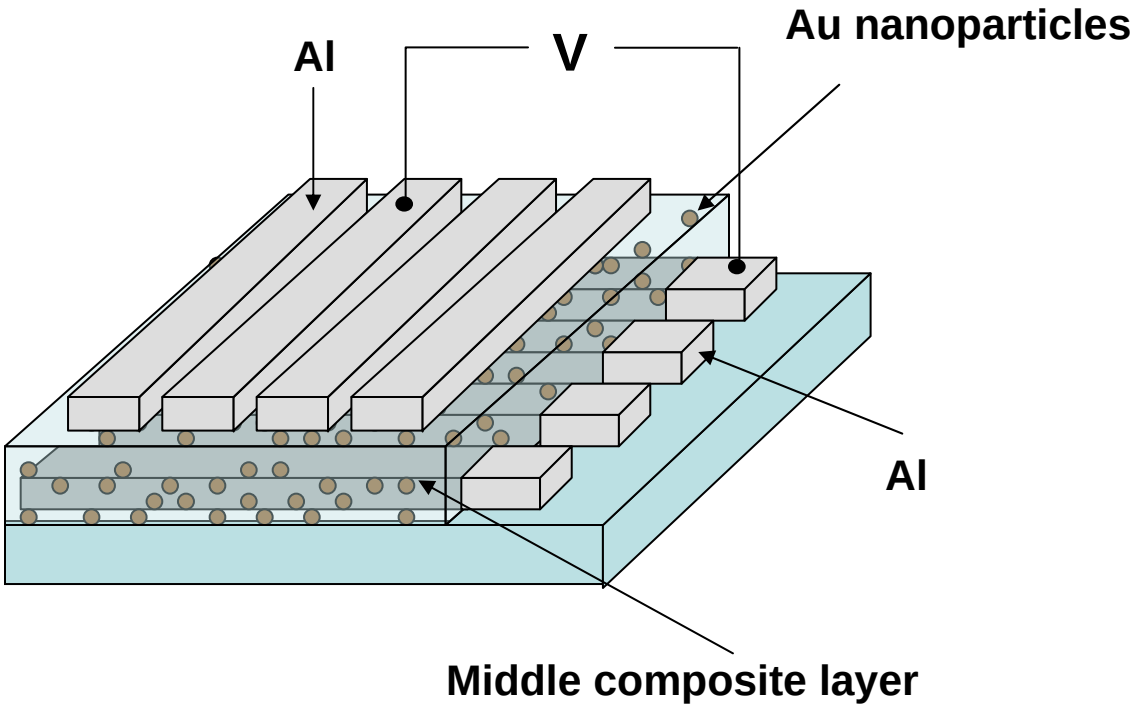

Figure 22.4 Device structure of an organic thin-film memory device.

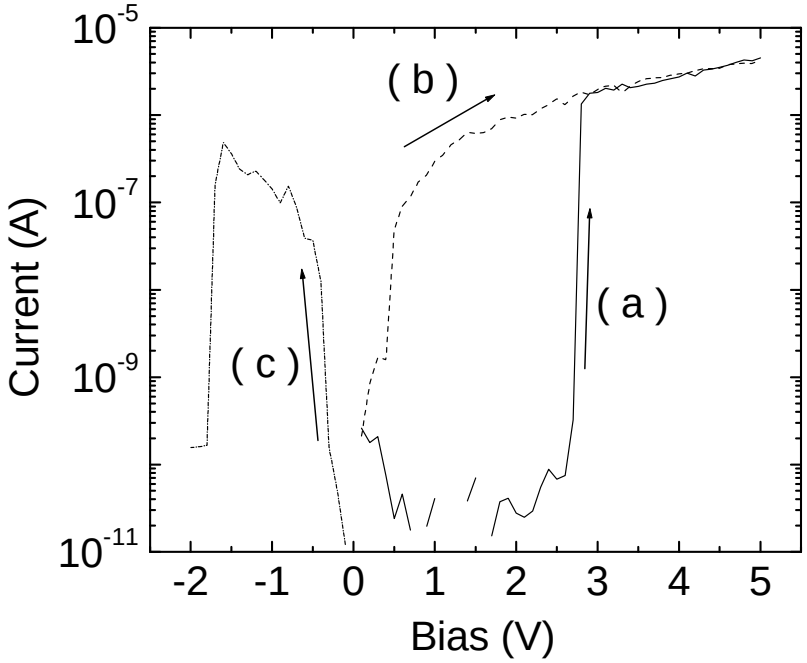

Figure 22.5 I-V curve of an organic memory device. (a), (b), and (c) represent the first, second, and third bias scans, respectively. The arrows indicate the voltage-scanning directions. (Reprinted from Ouyang, J., Chu, C.-W., Szmanda, C. Ma. L.P., and Yang, Y. *Nat. Mat.,* 3, 918, 2004. With permission. Copyright 2004 Nature Publishing Group.)

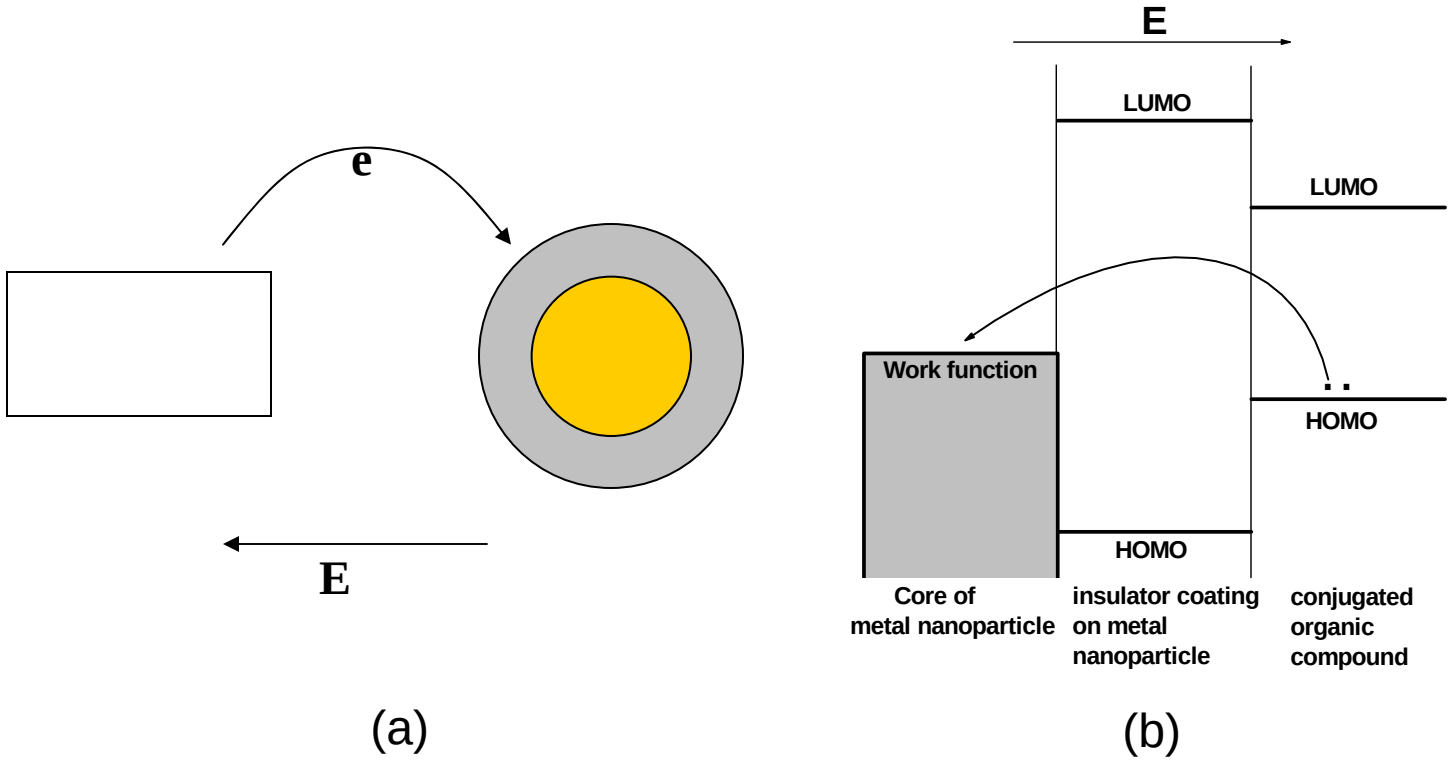

Figure 22.6 Schematic electron transfer from organic conjugated compound to the core of a metal nanoparticle. (a) The inner circle indicates the core of the metal nanoparticle, and the outer circle indicates the capped insulator layer. (b) The representative energy levels for organic compound and nanoparticle. The curved arrow denotes the electron transfer, and **e** denotes the electron. The direction of the electric field (**E**) is represented by the linear arrow.

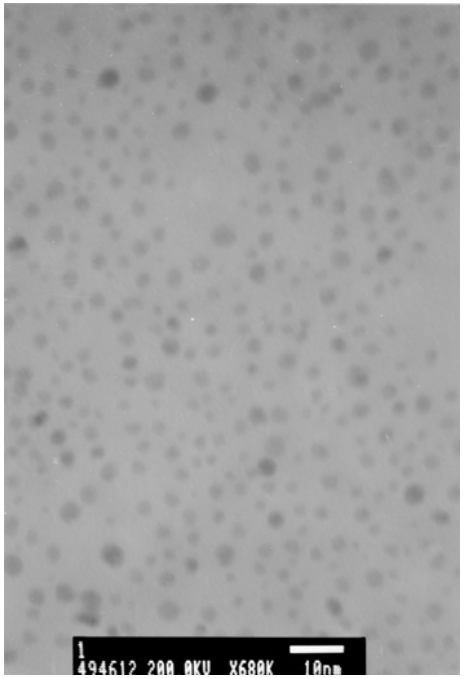

(a)

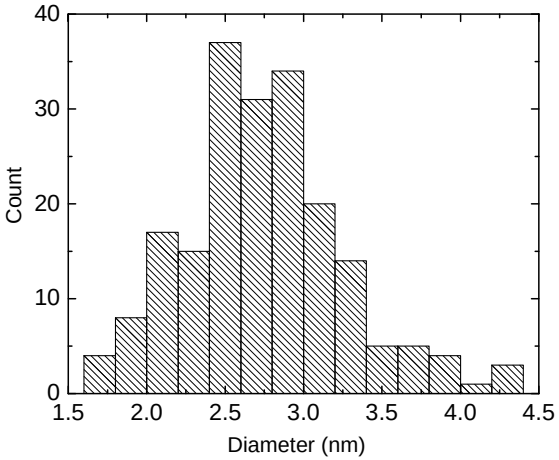

(b)

Figure 22.7 Transmission electron microscope (TEM) image (a) and size distribution hologram of metal nanoparticles (b). (Reprinted from Ouyang, J., Chu, C.-W., Szmanda, C. Ma. L.P., and Yang, Y. *Nat. Mat.,* 3, 918, 2004. With permission. Copyright 2004 Nature Publishing Group.)

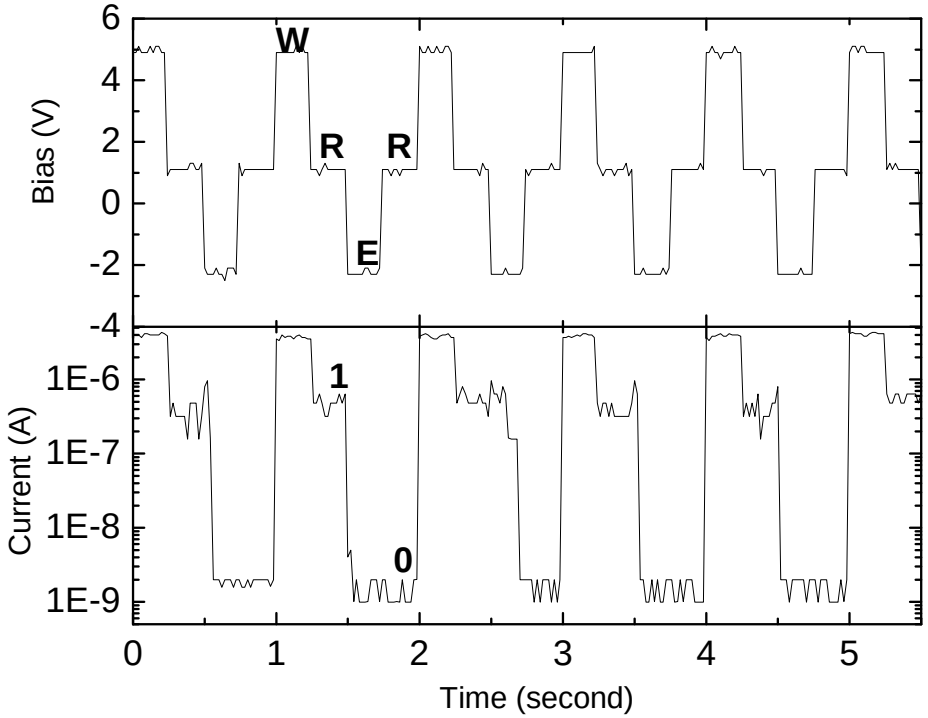

Figure 22.8 Write-read-erase cycles of device a polymer memory device. The top and bottom curves are the applied voltage and the corresponding current response, respectively. W, R, and E in the top figure mean write, read, and erase, respectively. “1” and “0” in the bottom figure indicate the device in the high and low conductivity state, respectively. (Reprinted from Ouyang, J., Chu, C.-W., Szmanda, C. Ma. L.P., and Yang, Y. *Nat. Mat.,* 3, 918, 2004. With permission. Copyright 2004 Nature Publishing Group.)

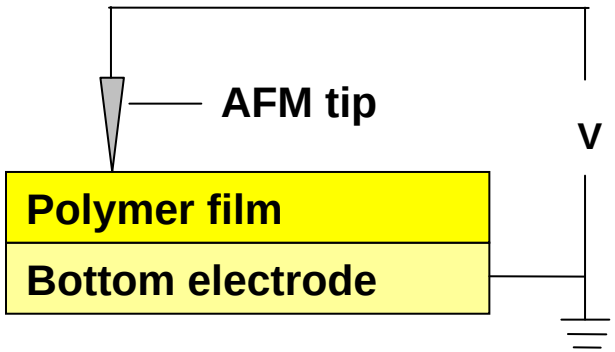

Figure 22.9 Test configuration for the operation of the device using an AFM tip as the top electrode.

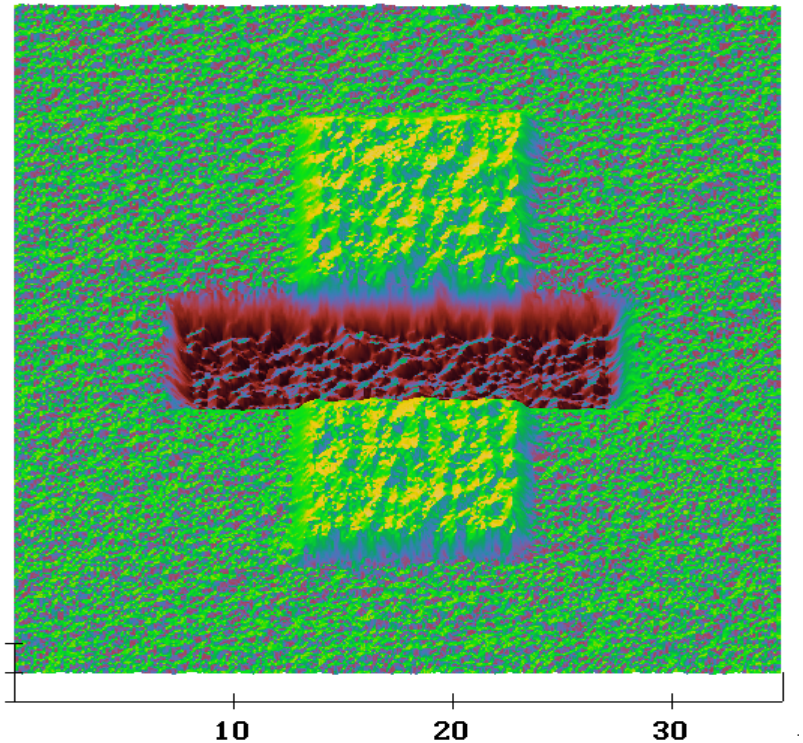

Figure 22.10 Scanning surface potential AFM image of a polystyrene (PS) film containing gold nanoparticle and 8-hydroxyquinoline (8HQ) with Al as bottom electrode and silicon wafer as substrate. The vertical bar with yellow color was pretreated with a +10 V dc bias, while the horizontal bar with brown color was pretreated with a -10 V dc bias. (Reprinted from Ouyang, J., Chu, C.-W., Szmanda, C. Ma. L.P., and Yang, Y. *Nat. Mat.,* 3, 918, 2004. With permission. Copyright 2004 Nature Publishing Group.)

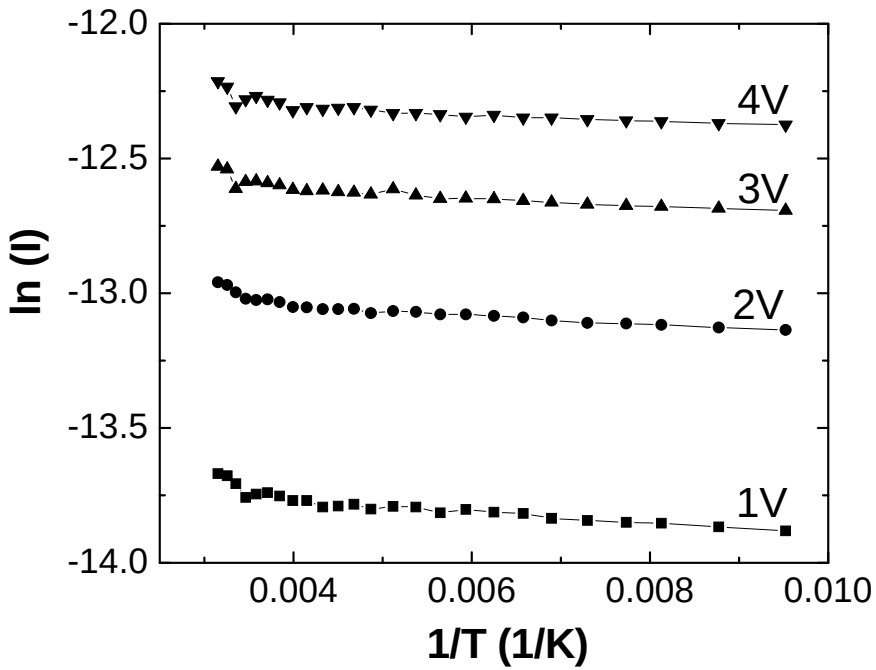

Figure 22.11 Arrhenius plot of temperature dependence of current for a polymer memory device in the high conductivity state at applied voltages of 1, 2, 3, and 4 V. (Reprinted from Ouyang, J., Chu, C.-W., Szmanda, C. Ma. L.P., and Yang, Y. *Nat. Mat.,* 3, 918, 2004. With permission. Copyright 2004 Nature Publishing Group.)

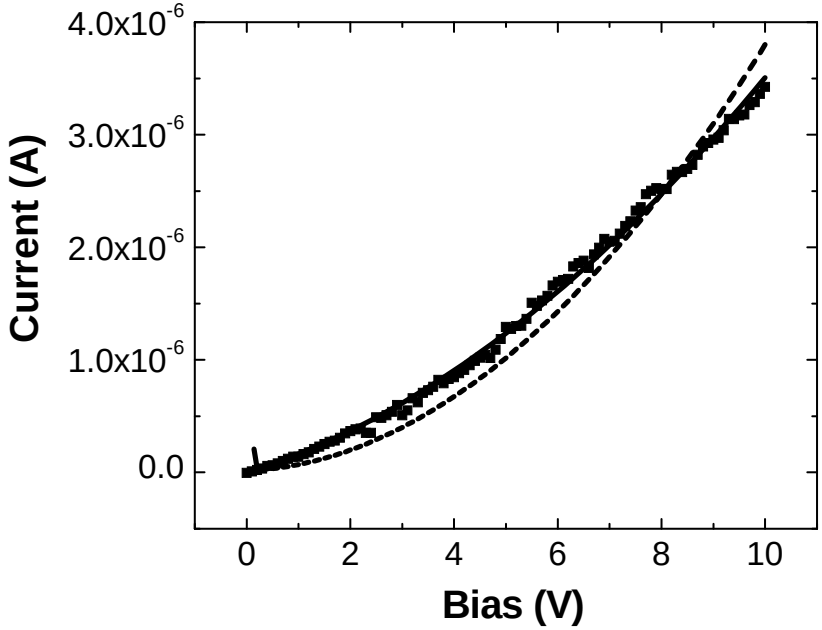

Figure 22.12 I-V curve of a polymer memory device in the high conductivity state. The scattered points are the experimental data, the solid line is the data fit combining direct tunneling and Fowler-Nordheim tunneling, and the broken line. (Reprinted from Ouyang, J., Chu, C.-W., Szmanda, C. Ma. L.P., and Yang, Y. *Nat. Mat.,* 3, 918, 2004. With permission. Copyright 2004 Nature Publishing Group.)